Molecular Therapy
Original Article

Enhancing CAR T function with the engineered secretion of *C. perfringens* neuraminidase

Joseph S. Durgin,[2,4] Radhika Thokala,[1,2] Lexus Johnson,[2,4] Edward Song,[2,4] John Leferovich,[2,4] Vijay Bhoj,[2,4] Saba Ghassemi,[2,4] Michael Milone,[2,4] Zev Binder,[1,3] Donald M. O'Rourke,[1,3] and Roddy S. O'Connor[2,4]

[1]Glioblastoma Translational Center of Excellence, The Abramson Cancer Center, Perelman School of Medicine at the University of Pennsylvania, Philadelphia, PA, USA; [2]Center for Cellular Immunotherapies, Perelman School of Medicine at the University of Pennsylvania, 3400 Civic Center Boulevard, Building 421, SPE 8-105, Philadelphia, PA, USA; [3]Department of Neurosurgery, Perelman School of Medicine at the University of Pennsylvania, Philadelphia, PA, USA; [4]Department of Pathology & Laboratory Medicine, Perelman School of Medicine at the University of Pennsylvania, Philadelphia, PA, USA

Prior to adoptive transfer, CAR T cells are activated, lentivirally infected with CAR transgenes, and expanded over 9 to 11 days. An unintended consequence of this process is the progressive differentiation of CAR T cells over time in culture. Differentiated T cells engraft poorly, which limits their ability to persist and provide sustained tumor control in hematologic as well as solid tumors. Solid tumors include other barriers to CAR T cell therapies, including immune and metabolic checkpoints that suppress effector function and durability. Sialic acids are ubiquitous surface molecules with known immune checkpoint functions. The enzyme *C. perfringens* neuraminidase (*CpNA*) removes sialic acid residues from target cells, with good activity at physiologic conditions. In combination with galactose oxidase (GO), NA has been found to stimulate T cell mitogenesis and cytotoxicity *in vitro*. Here we determine whether *CpNA* alone and in combination with GO promotes CAR T cell antitumor efficacy. We show that *CpNA* restrains CAR T cell differentiation during *ex vivo* culture, giving rise to progeny with enhanced therapeutic potential. CAR T cells expressing *CpNA* have superior effector function and cytotoxicity *in vitro*. In a Nalm-6 xenograft model of leukemia, CAR T cells expressing *CpNA* show enhanced antitumor efficacy. Arming CAR T cells with *CpNA* also enhanced tumor control in xenograft models of glioblastoma as well as a syngeneic model of melanoma. Given our findings, we hypothesize that charge repulsion via surface glycans is a regulatory parameter influencing differentiation. As T cells engage target cells within tumors and undergo constitutive activation through their CARs, critical thresholds of negative charge may impede cell-cell interactions underlying synapse formation and cytolysis. Removing the dense pool of negative cell-surface charge with *CpNA* is an effective approach to limit CAR T cell differentiation and enhance overall persistence and efficacy.

INTRODUCTION

Chimeric antigen receptor (CAR) T cells have become an important modality in cancer immunotherapy, producing a high rate of durable response for Food and Drug Administration-approved indications such as B cell acute lymphoblastic leukemia.[1,2] However, for solid malignancies, in which CAR T cells must contend with a complex, hostile, and often heterogeneous microenvironment, the results have been less encouraging. Most patients in clinical trials of CAR T for solid malignancies have had no objective response.[2] Moreover, even in relatively favorable indications such as hematologic malignancies, eventual disease progression is common. To overcome immunotherapy resistance, efforts have turned toward developing novel drugs and combination strategies to sensitize tumors to CAR T-mediated lysis. Among other approaches, the engineering of CAR T cells to produce effector proteins that block immune checkpoints, promote immune cell migration, and facilitate immune reactivity are exciting strategies on the frontier of immunotherapy research.[2]

The canonical immune checkpoints include inhibitory receptors such as CTLA4, PD1, and BTLA, which are expressed by T cells, and that serve to maintain peripheral tolerance and homeostatic contraction of T cell populations following immunologic stimulus.[3] However, following the discovery of immune checkpoint receptors, many other diverse mediators of peripheral tolerance have been discovered, including inhibitory cytokines, small molecule metabolites such as kynurenines, and cell-surface glycans.[4] For the latter category, the composition of glycans on mammalian cell surfaces has been shown to play a powerful role in modulating host-immune interactions. These discoveries have nominated promising therapeutic targets for enhancing immunotherapy. For example, glioblastoma cells were shown to overexpress truncated O-linked glycans that bind to the MGL receptor, which polarizes macrophages to an immunosuppressive phenotype.[5] Other glycan-binding receptors such as sialic acid-binding Ig-like lectins (siglecs) and dendritic cell (DC)-specific ICAM-3-grabbing nonintegrin 1 (DC-SIGN) have been shown to have roles in immune suppression.[6,7] Surface sialic acids, in particular, are appealing targets due to the manifold pathways in which

Received 16 April 2021; accepted 16 November 2021;
https://doi.org/10.1016/j.ymthe.2021.11.014.

Correspondence: Roddy S. O'Connor, PhD, Research Assistant Professor, Center for Cellular Immunotherapies, Perelman School of Medicine at the University of Pennsylvania, 3400 Civic Center Boulevard, Building 421, SPE 8-105, Philadelphia, PA 19104.
E-mail: oconnorr@pennmedicine.upenn.edu

they function as protective self-associated molecular patterns.[8] By binding to siglecs, sialoglycans trigger counterinflammatory cellular programs mediated by immunoglobulin receptor family tyrosine-based inhibitory motifs in the siglec cytoplasmic domains.[5,6] Siglec signaling on T cells can negatively modulate T cell receptor (TCR) signaling by reducing phosphorylation of Tyr^{319} on ZAP-70, one of the critical downstream mediators of both TCR and CAR signaling.[9] Beyond binding to siglecs, sialoglycans also mediate immune inhibition by reducing cell-cell interactions through electrostatic repulsion, disabling the contents of T cell cytotoxic granules, and inhibiting complement activation.[10–12] Concordantly, diverse cancer types have been shown to highly express surface sialic acid, and this overexpression has been associated with worse clinical outcomes.[8,10,13,14]

The targeting of sialoglycans for cancer pharmacotherapy is a relatively old concept, predating our understanding of their mechanisms as immune checkpoint effectors. Treatment of tumor cells with sialic acid-cleaving neuraminidase enzymes was demonstrated in mouse and canine models to potentiate immune recognition of both treated and nontreated cells.[15–17] Neuraminidases (NAs) are produced by diverse species including *Vibrio cholerae*, *Clostridium perfringens*, influenza viruses, and mammals.[18] While the initial studies of NA-treated tumor cells were encouraging, a randomized, controlled trial in colorectal cancer published in 1989, using subcutaneous injection of *Vibrio cholera* neuraminidase (VCN)-modified autologous tumor cells, found no benefit for progression-free or overall survival over 5 years, a setback in the nascent field of immunotherapy.[19]

However, as our understanding of sialoglycans as immune checkpoints has advanced, there is now renewed interest in targeting these structures in cancer therapy. Promising next generation strategies have included an engineered adenovirus expressing the hemagglutinin-NA of Newcastle Disease Virus, which reduced tumor sialic acid content and promoted disease regression *in vivo*.[20] More recently, a sialidase-conjugated antibody-like polymer targeting PD-L1 demonstrated both *in vitro* and *in vivo* efficacy against the MDA-MB-231 mammary adenocarcinoma.[21]

We hypothesized that CAR T cells engineered to express a highly active, secreted neuraminidase would be a more potent immunotherapeutic strategy than CAR T alone in solid tumors. We engineered epidermal growth factor receptor (EGFR) and CD19-directed CAR T cells to secrete functional *C. perfringens* NA. The *C. perfringens* NA was chosen due to having a pH optimum in the range of 6.5 to 7.2, closer to the physiological range of human extracellular fluid when compared with the NA of the enteric pathogen *Vibro cholerae* (optimum pH of 5.5–6.0) or the human NAs that are optimized for acidic compartments (optima of 4.4–4.6 for lysosomal Neu1, 6.0–6.5 for the cytosolic Neu2, 4.6–4.8 for Neu3, and 3.5 for lysosomal Neu4).[22–24] The influenza NA was not suitable, as adults and the elderly often have high titers of anti-influenza NA antibodies due to past virus exposure.[25]

Interestingly, the work of Novogrodsky with NA also demonstrated that its combination with the enzyme galactose oxidase (GO) can activate T cell mitogenesis and cytotoxicity more so than NA alone.[26,27] The enzyme GO oxidizes the galactose residues revealed by NA's uncapping of terminal sialic acids, creating reactive galactose aldehydes. These reactive groups have been hypothesized to account for the mitogenic effect of the NAGO combination by cross-linking cell-surface glycoproteins in a lectin-like manner.[27] The proinflammatory effect of the NAGO combination has made it an effective vaccine adjuvant in animal studies, promoting immunologic memory as measured by antiparasitic immunity and delayed hypersensitivity reactions to antigen reexposure.[28] While mitogen activation of T cells also risks overstimulation, inviting exhaustion and activation induced cell death, there has also been some evidence that stimulating T cell activation outside of the tumor microenvironment can promote immunotherapeutic response. For example, Reinhard et al. co-treated mice with large syngeneic LL/2-LLc1 or CT26 tumors using CAR T cells in combination with an RNA vaccine encoding the claudin target antigen.[29] By introducing target antigen outside of the tumor, this strategy allowed the CAR T product to establish a foothold in more permissive environments prior to engaging with the tumor microenvironment. It seemed reasonable to suppose that the combination of NA and GO might similarly augment tumor lysis beyond the antitumor effects of interfering with sialoglycan checkpoint pathways alone.

We explored the potential of *C. perfringens* NA-producing T cells, either alone or combined with GO, to promote CAR T mediated tumor lysis. The mechanisms of NA and GO stimulation of T cells, being previously poorly defined, were probed with CRISPR knockouts to reveal the importance of the CD2 adhesion and costimulatory receptor in this therapeutic approach. We demonstrate *in vivo* that *Cp*NA secreting CAR T cells exert better control than conventional CAR T alone, but the addition of exogenous GO produces no further benefit despite its promise in *in vitro* assays. Secretion of *CpNA* led to enriched naïve-like differentiation of CAR T cells during *ex vivo* expansion, a phenotype that is associated with greater persistence and activity of the therapeutic product *in vivo*, suggesting that cleaving surface sialic acids influences T cell differentiation in addition to modulating checkpoint pathways.[30–32] In the design of novel immunotherapies, the targeting of tumor and immune cell-surface glycans to enhance immunogenicity, such as through the glyco-active enzyme NA, has the potential to enhance CAR T efficacy against solid tumors.

RESULTS

Engineered CAR T cells secrete functional *Cp*NA in an antigen-responsive manner

To study the potential role of NA as a secreted factor that enhances CAR T cell antitumor function, we generated the lentiviral vector GFP_T2A_NA (GTN) by cloning the *C. perfringens* neuraminidase (*Cp*NA) into a pTRPE plasmid backbone containing enhanced GFP (eGFP) and the T2A self-cleaving peptide (Figure 1A). After overnight stimulation with Dynabeads, activated T cells were co-transduced with GTN and either 806 (an EGFR-specific, 4-1BBZ CAR)

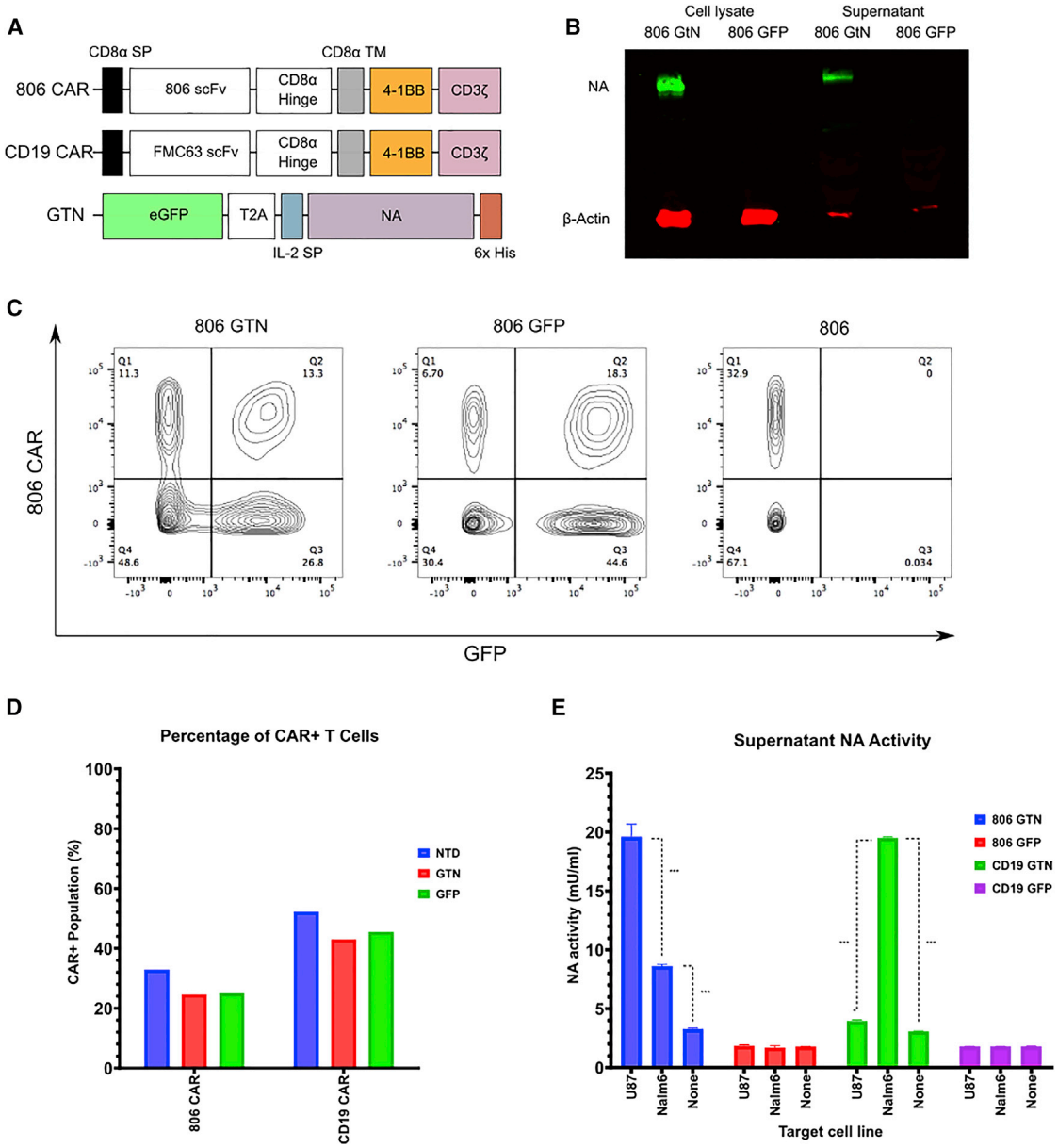

Figure 1. Engineering CAR T cells to secrete functional *Clostridium perfringens* neuraminidase (*Cp*NA)

(A) Schematic representation of the hEGFR lentiviral CAR containing an 806 scFv, which is linked via a CD8alpha hinge as well as a CD8a TM to the 4-1BB and CD3zeta intracellular signaling domains. SP, signal peptide; TM, transmembrane. A lentiviral CAR construct against human CD19 containing the FMC63 scFv is also shown. GTN is a bicistronic lentiviral construct expressing *C. perfringens* neuraminidase (*Cp*NA) in tandem with a C-terminal 6× Histidine tag (6× His) as well as the transduction marker GFP. (B) After overnight stimulation with Dynabeads, T cells were co-infected with an EGFR CAR and GTN lentiviral supernatants. These cells were expanded for 3 days. Cellular lysates and supernatants were collected and immunoblotted with anti-His antibody. Relative protein loading was determined by immunoblotting for B-Actin. Representative data from two independent experiments are shown. (C) *Cp*NA-expressing CAR T cells were generated as in (B) Surface EGFR CAR expression was measured by staining with a recombinant EGFRvIII-Fc protein (H + L) followed by anti-Fc-APC labeling. GTN levels were simultaneously detected by GFP expression. CAR + cells were defined as double-positive for *Cp*NA (x axis) and PE (y axis). Representative flow plots from three independent experiments are shown. (D) The percentage of T cells positive for CAR expression after preparation as in (C). Representative data from one of three donors are shown. (E) CAR T cells were co-cultured with either U87-MG or Nalm6 tumor cells at a 10:1 ratio for 24 h. Cellular supernatants were collected and NA enzymatic activity was detected as described in the materials and methods. The mean ± SEM values of three independent experiments with separate donors are shown. Data were analyzed with pairwise t tests corrected for multiple comparisons using the Holm-Sidak method. ***$p < 0.001$ for CAR T cells co-cultured with tumor cells expressing the CAR's target antigen versus control cells expressing an irrelevant antigen.

or CD19-specific, 4-1BBZ CAR lentivirus. As a control, T cells were transduced with eGFP lentivirus instead of GTN. After 3 days, cellular lysates and supernatants were collected and *Cp*NA expression was confirmed by western blot with antibodies against the C-terminal 6× histidine tag (Figure 1B). The *Cp*NA secreting CAR T cells expanded efficiently (25.4-fold, Figure S1A), although more slowly than GFP-transduced controls, with 45.3% fewer total T cells at the end of expansion (defined by median cell size <400 fL) across three donors ($p = 0.016$). As sialic acids have been implicated in protecting immune effector cells from degranulation-associated self-killing,[11] we examined T cell viability at consecutive time points during expansion (Figure S1B). By live dead staining, there was a greater proportion of dead cells in the *Cp*NA secreting condition versus the GFP control, with 20.7% versus 12.5% dead cells on day 3, 11.8% versus 4.2% on day 5, and 4.4% versus 1.4% on day 7, but these differences were not significant by paired t test statistics with three donors ($p = 0.1172$, 0.1147, and 0.0858 on days 3, 5, and 7, respectively).

To evaluate *Cp*NA expression in CAR + subsets, we performed two-color flow cytometry with GFP positivity indicating transduction with the GTN construct. After dual transduction with CAR and GTN lentiviral preparations, we observed a mix of singly positive CAR, GTN, and CAR + GTN T cells (Figures 1C and 1D). The CAR + transduction efficiencies were comparable in the GTN (24.6%) and GFP (25%) populations and similar to the targeted CAR + percentage in clinical products.[33] To evaluate whether *Cp*NA production confers a relative growth disadvantage to T cells producing it, we examined GFP positivity as a proxy for *Cp*NA expression at serial time points during expansion (Figure S1C). By paired t testing across three donors, there was no significant decrease in GFP percent positivity between days 3 and 7 ($p = 0.4755$) in the *Cp*NA condition, suggesting that the decrease in *ex vivo* expansion related to NA is due to its effects on the population and not limited to cells expressing the enzyme.

To test how *Cp*NA secretion responds to CAR stimulation, we selected target lines U87 and Nalm6 with EGFR and CD19 positivity, respectively. Activated T cells were co-infected with GTN and CAR, expanded for 10 days, and frozen before use. CAR T cells were then co-cultured with either U87 or Nalm-6 target cells for 24 h at a 10:1 effector to target cell (E:T) ratio.

Cellular supernatants were collected and *Cp*NA activity was determined with a cleavage-activated fluorescent NA substrate. We show that *Cp*NA activity is significantly induced following direct stimulation of the CAR with its corresponding ligand. As shown in Figure 1E, *Cp*NA levels/activity significantly increased 2.3-fold from 8.62 to 19.63 mU/mL ($p = 0.0001$) when GTN 806 CAR T cells were co-cultured with U87 versus Nalm6 cells, respectively. Similarly, *Cp*NA functional activity increased 4.9-fold from 3.96 to 19.52 mU/mL ($p < 0.0001$) when GTN CD19 CAR T cells were co-cultured with Nalm6 versus U87, demonstrating that enzyme secretion is enhanced after CAR-mediated T cell activation.

CAR T-secreted *Cp*NA enhances T cell-mediated tumor lysis *in vitro*

We hypothesized that CAR T cells secreting *Cp*NA would have enhanced tumor lysis compared with CAR T cells alone. As Novogrodsky found that GO in the presence of NA induced T cell mitogenesis, we also hypothesized that adding GO to *Cp*NA secreting CAR T cells would confer additional antitumor function.[27] To rule out direct toxic effect of the enzymes on tumor cell lines, we initially examined whether NA and GO inhibit the growth of U87 or Nalm6 cells in the absence of T cells. Using luciferase-expressing tumor cells, we showed that the addition of exogenous *Cp*NA and GO, in the absence of T cells, did not inhibit growth of either tumor line (Figure 2A). To determine the effective range of GO doses that stimulate T cell-induced lysis in combination with *Cp*NA secreting CAR T cells, we co-cultured GTN or GFP CD19 CAR T cells with U87 cells at a 1:1 ratio for 24 h. In the absence of *Cp*NA, exogenous GO at higher doses (375 mU/mL) induced nonspecific lysis of U87 cells by GFP CD19 CAR T cells (Figure 2B). However, *Cp*NA-expressing GTN CD19 CAR T cells produced significantly greater lysis of U87 cells compared with GFP-transduced CD19 CAR T cells after the addition of GO, with a 4.4-fold, 3.3-fold, and 1.6-fold increase in tumor cell lysis at GO doses of 3.75, 37.5, and 375 mU/mL, respectively (Figure 2B, $p = 0.0053$, <0.0001, and 0.0001).

To assess whether secreted *Cp*NA, alone or in combination with GO, enhances the ability of CAR T cells to lyse their corresponding target cells, we co-cultured GTN and GFP CAR T cells with U87, U251, or Nalm6 target cells. CAR T cells were expanded for 10 days until rested, and then co-cultured with target cells at various effector to target (E:T) ratios for 24 h. In the absence of exogenous GO, the cytolytic activity of GTN and GFP CAR T cells against U87 cells is similar (Figures 2C and 2D). However, the addition of exogenous GO potentiated U87 cell lysis by *Cp*NA-expressing CAR T cells, leading to a 2.47-fold increase in tumor lysis at the 1:3 ET ratio compared with *Cp*NA secreting CAR T cells alone (Figure 2C, $p = 0.0024$). For U251 and Nalm6 cells, the *Cp*NA secreting CAR T cells alone outperformed control GFP-transduced CAR T cells. With U251 targets, *Cp*NA secretion produced a 1.27- and 1.7-fold increase in lysis at ET ratios of 1:1 and 1:3, respectively (Figure S2A, $p = 0.0035$ and 0.0347). With Nalm6 targets, *Cp*NA secretion by CD19-directed CAR T cells produced a 2.5- and -3.9-fold increase in lysis at ET ratios of 3:1 and 1:1, respectively (Figure S2D, $p = 0.0006$ and 0.0053). For both U251 and Nalm6 targets, the addition of GO further enhanced lysis compared with *Cp*NA secreting CAR T cells alone, with 1.7- and 3.3-fold increases in tumor lysis, respectively, at an ET ratio of 1:3 (Figure S2, $p = <0.0001$ and 0.0098).

By ELISA assay, interferon (IFN)-γ and interleukin (IL)-2 cytokine levels were significantly increased in the CAR T and tumor co-cultures in the presence of secreted *Cp*NA and exogenous GO (Figures 2E and 2F), even with an irrelevant CD19-directed CAR, showing that *Cp*NA secretion plus exogenous GO leads to antigen-independent T cell reactivity and TH1 cytokine production.

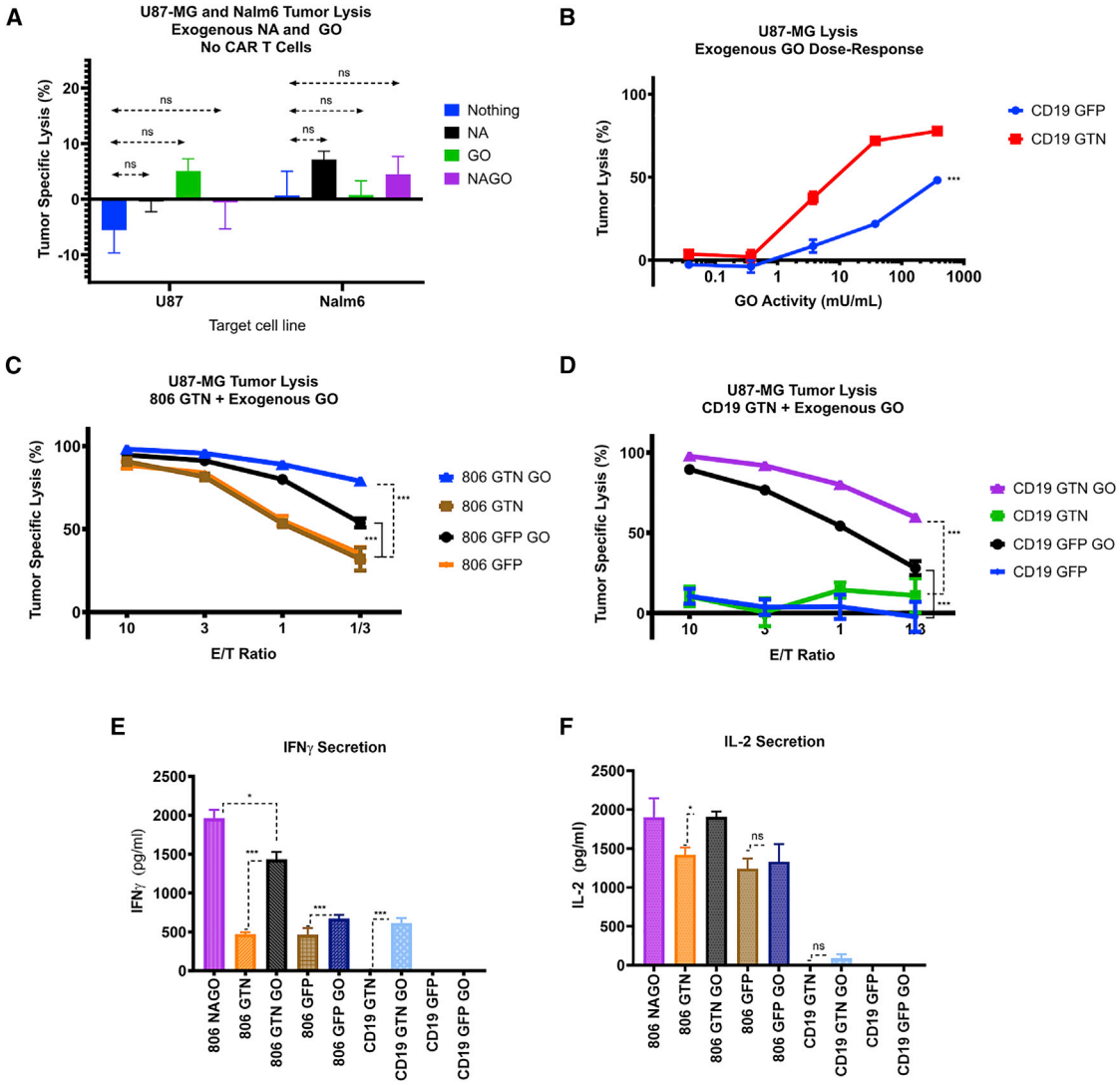

Figure 2. The combination of CAR T-secreted *Cp*NA and exogenous galactose oxidase (GO) enhances T cell-mediated tumor lysis of U87 cells

(A) U87-MG as well as Nalm6 tumor cells were treated with exogenous *Cp*NA and GO for 24 h. Tumor cell lysis was measured by luciferase assay. p = 0.31 for enzyme effect on cell proliferation by a one-way ANOVA using a Tukey multiple comparison correction. (B) CD19-directed CAR T cells were co-cultured with U87 target cells. The media was conditioned with exogenous GO at various concentrations, and U87-MG tumor lysis was assessed via bioluminescence at 24 h. (C) T cells were co-infected with an EGFR-specific CAR and either GFP or *Cp*NA lentiviral supernatants. The CAR T cells were co-cultured with luciferase-expressing U87-MG target cells, in medium conditioned with exogenous GO. After 24 h, cytotoxicity across a range of E:T ratios was measured by a luciferase-based killing assay. Values are mean ± SEM. A representative experiment from three independent replicates with separate donors is shown. ***p = 0.0002 for 806 GTN GO versus 806 GTN at a 1:1 E:T ratio; **p = 0.0024 for 806 GTN GO versus 806 GTN at a 1:3 E:T ratio. (D) Tumor cell lysis was measured as in (C), but anti-CD19 CAR T cells were used instead of anti-EGFR CAR T cells. ***p = 0.0002 for CD19 GTN GO versus CD19 GTN at a 1:1 E:T ratio; *p = 0.0108 for CD19 GTN GO versus CD19 GTN at a 1:3 E:T ratio. (E) CAR T cells, coexpressing either GFP or *Cp*NA were treated with exogenous galactose oxidase for 24 h. Cellular supernatants were collected and IFNγ levels were detected by ELISA. (F) IL-2 levels in 24 h supernatants as detected by ELISA.

With light microscopy, we observed that the presence of *Cp*NA led to greater cell-cell association between T cells and tumor cells in co-cultures (Figures S3A and S3B). While co-cultures without NA had many T cells that were not engaged in clusters with tumor targets, the cultures with *Cp*NA had comparatively few unengaged T cells (Figures S3A and S3B). The ability of NA to promote cell-cell adhesion has been previously demonstrated and has been hypothesized by others to explain its pro-immunogenic effect.[10]

*Cp*NA and GO-mediated T cell activation depends on the CD2:CD58 signaling axis

The mechanism by which the *Cp*NA and GO combination acts as T cell mitogens remains incompletely described. Novogrodsky

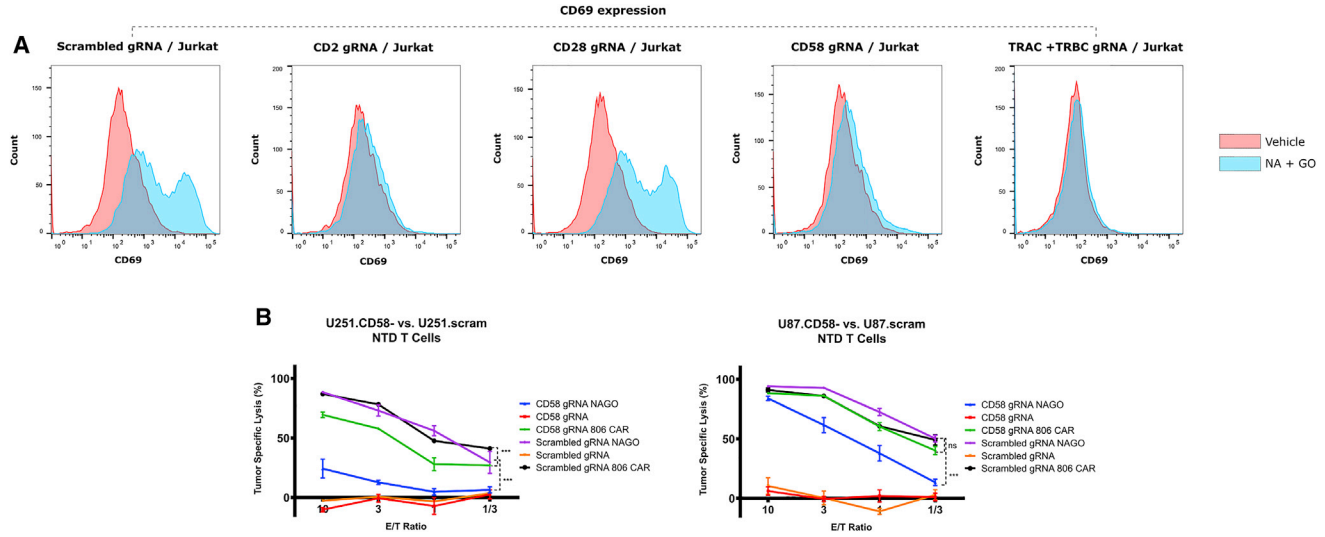

Figure 3. The combination of *Cp*NA and GO activate T cells and promote tumor lysis in a CD2:CD58-dependent manner

(A) Jurkat cells were infected with the lentiCRISPR-v2 system adapted with gRNAs for *CD2*, *CD28*, *CD58*, the T cell receptor alpha and beta chains (*TRAC* and *TRBC*), and a scrambled nontargeting control. The cells were selected with puromycin and knockout confirmed by flow cytometry 5 days after transduction. After an overnight incubation with NA and GO, the cells were stained with APC-conjugated anti-CD69 antibody and assessed by flow cytometry. (B) Luciferase expressing U87 and U251 cells were infected with the lentiCRISPR-v2 system encoding gRNAs against CD58 or a scrambled sequence. Knockout was confirmed after 5 days. The target cells were plated at 20×10^3 per well and co-incubated with nontransduced or 806 CAR T cells at E:T ratios of 10:1, 3:1, 1:1, or 1:3. Wells with nontransduced T cells were treated with NA and GO (50 mU/mL and 375 mU/mL, respectively) or PBS vehicle. Tumor lysis was determined by bioluminescence assessment after 24 h. Data are means ± SEM, showing a representative experiment from three replicates with separate donors.

hypothesized that free amines may attack the GO- generated reactive aldehydes in a Schiff base reaction, leading to covalent cross linking of cell-surface receptors and transmission of activating signals.[27] However, the precise receptors involved in transmitting the activating signals are unknown. A report by Ocklind et al. demonstrated that anti-CD2 or CD58 monoclonal antibodies could block the formation of rosettes between human T cells and sheep erythrocytes in the presence of *Cp*NA and GO.[34] We hypothesized that eliminating CD2 or CD58 expression would abrogate the effects of *Cp*NA and GO on T cell activation and tumor cell lysis.

We adapted the lentiCRISPR-v2 system of Sanjana et al. with guide RNAs (gRNAs) for *CD2*, *CD28*, *CD58*, *TRAC*, *TRBC*, and a scrambled control.[35] After producing lentiviral particles, we transduced Jurkat cells, a T cell leukemic line commonly used in investigations of TCR and CD2 signaling. We confirmed gene knockout by flow cytometry 5 days later (Figure S4). To assess activation of the cells after overnight *Cp*NA and GO stimulation, we measured expression of CD69, a marker of T cell activation.[36] These data show that Jurkat cells deficient in CD2, CD58, or the TRC chains TRAC and TRBC are not activated by *Cp*NA and GO treatment (Figure 3A).

Conversely, the loss of CD28 or expression of a nontargeting gRNA did not affect the response to the enzymes (Figure 3A). Therefore, CD2, its ligand CD58, and the TCR are required for *Cp*NA and GO in combination to activate Jurkat cells.

Based on the CRISPR knockout data, we suggest that Jurkat cells are activated in the presence of *Cp*NA and GO through complementation of CD2 and its ligand CD58 expressed on neighboring cells. The requirement for the TCR is due to its role in transmitting signals from the CD2 axis.[37] If the enzymes do act through CD2-CD58 complementation, then CD58 expression on tumor cells may contribute to their *Cp*NA and GO-mediated lysis. Using the lentiCRISPR-v2 constructs, we transduced luciferase-expressing U87 and U251 tumor cells with CD58 or scrambled gRNAs and confirmed knockout 5 days later (Figure S4). We co-cultured these cells with nontransduced T cells at various E:T ratios, with and without exogenous *Cp*NA and GO, for 24 h and determined cell lysis with bioluminescence assay. These data show that CD58-deficient tumor cells are resistant to NA- and GO-stimulated T cell cytotoxicity, with tumor-specific lysis decreasing 47.8% ($p = 0.0081$) and 91.7% ($p = 0.00053$) for U87 and U251 cells, respectively, when CD58 is knocked out (Figure 3B, values for ET = 1). In parallel experiments, we included EGFR-directed CAR T cells to examine whether CD58 knockout confers resistance to CAR-stimulated lysis. We found that CAR T cell-mediated lysis was not significantly inhibited in CD58 deficient tumor cells, with reductions of 0.06% ($p = 0.92$) and 41.3% ($p = 0.092$) compared with scrambled gRNA transduced cells (Figure 3B, values for ET = 1), suggesting that loss of CD58 confers resistance to NA and GO-mediated lysis specifically instead of only providing a general resistance to T cell cytotoxicity.

*Cp*NA secretion confers naïve-like differentiation to T cell cultures *in vitro*

Differentiation status is an important determinant of CAR T cell efficacy. Therefore, we performed a comprehensive assessment of differentiation using well-established surface markers. We show that *CpNA*-expressing T cells possess significantly higher levels of naïve-like subsets at the end of the *ex vivo* culture process (Figures S5A and S5B). Importantly, levels of naïve-like cells provide the most meaningful predictors of efficacy in CAR T cell trials, with superior engraftment, proliferation, and persistence following infusion. These differentiation data suggest that one mechanism for enhanced *CpNA*-expressing CAR T performance *in vivo* may be enhanced durability and long-term immunosurveillance.

*Cp*NA secretion enhances CAR T activity against U87 solid tumors and Nalm6 leukemia *in vivo.*

Based on the *in vitro* findings, we hypothesized that CAR T cells secreting *Cp*NA would better eradicate xenografted solid tumors in mice compared with CAR T cells alone, and that exogenous GO may further augment this benefit. We generated anti-EGFR and anti-CD19 CAR T cells as previously described, co-transduced with either the GTN (*Cp*NA secreting) or GFP constructs. Each mouse received 250×10^3 luciferase-expressing U87 tumor cells via subcutaneous injection in the flank (Figure 4A). On day 7, the tumors were palpable, and the mice received 500×10^3 CAR T cells in PBS each by tail vein injection. On days 8 and 21, the mice received 30 μL of GO (37,500 mU/mL in PBS) or vehicle by intra-tumoral injection. On a weekly basis, the tumor volume and bioluminescence were assessed with caliper measurements and the IVIS Spectrum imaging system, respectively. In animals receiving the irrelevant CD19-directed CAR T cells, the best tumor control occurred with *Cp*NA secreting CAR T cells plus GO injections, which produced a 42.7% ($p = 0.0474$) and 66.3% ($p = 0.0069$) reduction in tumor bioluminescent imaging (BLI) at days 21 and 28, respectively, compared with the next best treatment (Figure 4B). This suggests NA and GO may have stimulated T cell activation and lysis of the tumor. However, by day 35, 2 weeks after the last injection of GO, the *Cp*NA secreting CAR T plus GO arm was no longer significantly better than other conditions (Figure 4B, $p = 0.9800$). In 806 CAR T treated animals, the *Cp*NA secreting T cells controlled the tumor significantly better than all other conditions, with an 85.9% lower tumor BLI compared with the next best treatment at the final time point (Figure 4D, $p = 0.0005$). However, 806 GTN CAR T-treated animals that received injected intra-tumoral GO did worse than those receiving PBS (Figure 4D, $p = 0.0005$). The mice showed no evidence of accelerated graft versus host effect either by physical inspection or serial weights. Overall, the secretion of *Cp*NA by EGFR-targeting CAR T cells led to enhanced tumor control, while producing no adverse effects in the mice (as assessed by weight, blood counts, and serum chemistries). The addition of GO, however, did not further benefit animals receiving *Cp*NA secreting EGFR-targeting CAR T cells.

Mechanistically, our *in vitro* assays had revealed that *Cp*NA secreting CAR T cells possessed a more naïve-like ($CCR7^+CD45RO^-$ with slower expansion) phenotype. As naïve-like T cells have been demonstrated to confer superior persistence and longer-lasting immunosurveillance against hematologic malignancies, we used an NSG mouse/Nalm6 tumor rechallenge model to test the hypothesis that *Cp*NA secreting CAR T cells would produce more durable tumor control. Each mouse (five per cohort) received 1×10^6 luciferase-expressing Nalm6 tumor cells by tail vein injection (Figure 5A). On day 5, we infused *Cp*NA secreting versus GFP control CD19-directed CAR T cells. On day 33, mice received an additional 1×10^6 Nalm6.GFP/Luc cells by tail vein injection. By day 50, mice treated with the *Cp*NA secreting CAR T cells had a greater than 1,000-fold lower tumor burden than those treated with control CAR T cells (*$p = 0.0163$, Figure 5B) Concordantly, 80% of mice in the *Cp*NA CAR T group survived until the end of the experiment versus 0% survival in the GFP control group (*$p = 0.0210$, Figure 5C). Blood was collected on day 44, and while the *Cp*NA CAR T group did demonstrate 350-fold higher levels of human CD45 + engrafted lymphocytes, this result was not significant perhaps due to low sample size secondary to mortality in the GFP group ($p = 0.3372$, Figure 5D). Two weeks after tumor rechallenge, the BLI of the *Cp*NA CAR T group started to decrease, indicating tumor regression, and by the last measurement on day 50 the tumor burden in that group was barely detectable (Figure 5E).

*Cp*NA secretion enhances CAR T activity against B16 melanoma but not the SY5Y neuroblastoma model

As *in vitro* studies suggest that GO adds to the effect of NA by facilitating activation of *in situ* T cells through CD2:CD58, we hypothesized that the absence of an endogenous immune system in NSG mice might account for the lack of enhancement of *Cp*NA CAR T-mediated lysis after addition of GO. To test the system in an immune-competent model, we implanted C57BL/6 mice with syngeneic B16F10 tumor cells expressing human CD19. Mice were randomized to treatment on days 5 and 12 with CD19-directed CAR T cells, co-transduced with GTN or GFP constructs, or NTD controls (Figure S6A). Mice also received intra-tumoral injections of NA and GO, GO, or PBS vehicle on days 6 and 13 as indicated in figures. Similar to the NSG experiment, we saw the best tumor control in the *Cp*NA CAR T plus PBS injection treatment arm, with a 42.8% reduction in tumor volume by day 21 compared with NTD- and PBS-treated animals ($p = 0.0126$) and 33.3% reduction compared with the *Cp*NA CAR T plus GO treatment arm (Figure S6B), although the latter was not significant ($p = 0.0667$). Analyzing blood collected on day 21, we saw engraftment of CD45.1+ adoptively transferred T cells in all treatment arms, although as assessed by one-way ANOVA with corrections for multiple comparisons, there were no significant differences between arms (Figure S6C, $p = 0.0642$). Assessment of weights by two-way ANOVA (mixed effects model) showed no significant treatment or time-treatment interaction effects (Figure S6D, $p = 0.2635$ and 0.0598, respectively). Overall, in this syngeneic solid tumor model, we observed superiority of *Cp*NA secreting CAR T cells but an absence of improvement with additional exogenous GO.

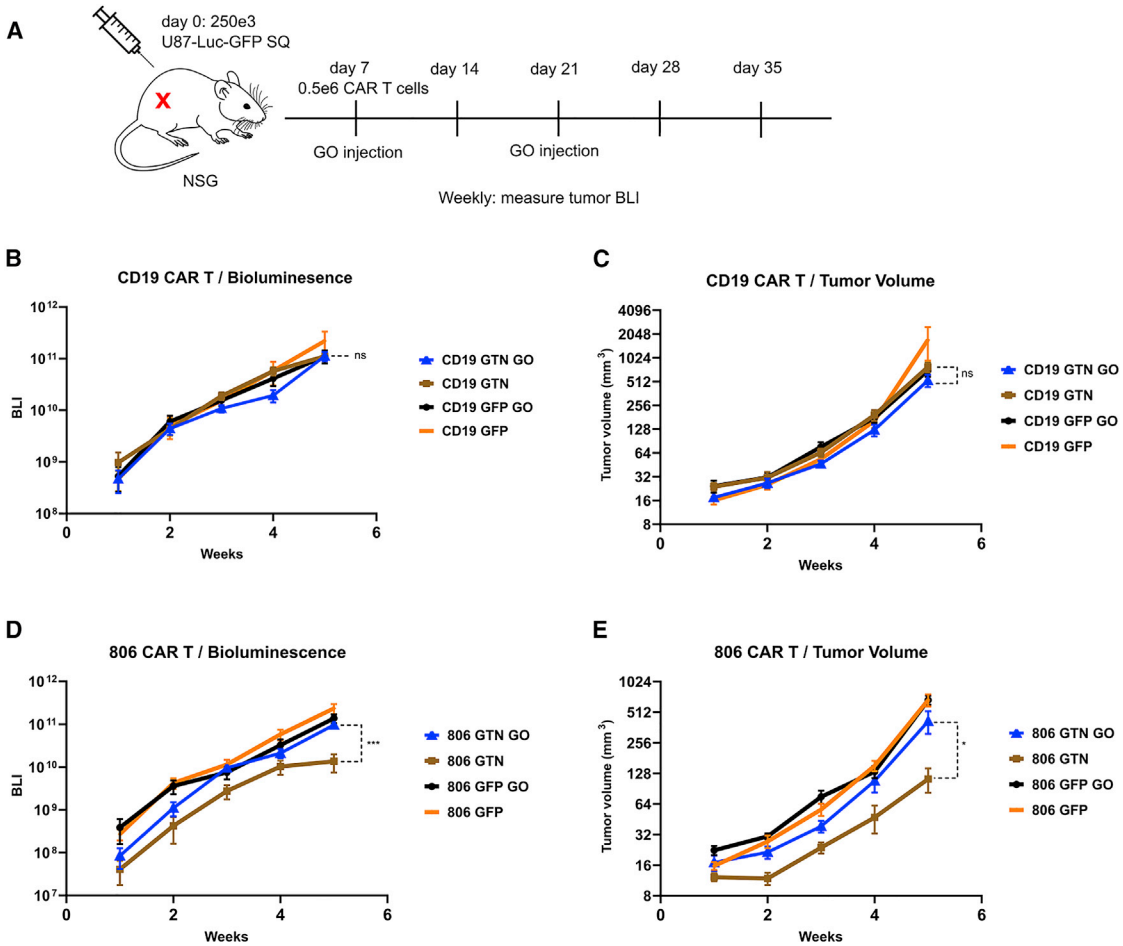

Figure 4. Tumor bioluminescence in NSG mice after implantation with U87 tumor cells and treatment with *CpNA* secreting CAR T cells

(A) NSG mice were implanted by subcutaneous flank injection with 250 × 10^3 luciferase-expressing U87 tumor cells. On day 7, the mice received 500 × 10^3 CAR T cells in PBS injected by tail vein. The CAR T cells expressed 806 (EGFR-targeting) or anti-CD19 CARs plus co-transduced GTN (CpNA secreting) or GFP constructs. On days 8 and 21, the mice received 30 mL of GO (37,500 mU/mL in PBS) or vehicle by intra-tumoral injection. Every seventh day, the tumor bioluminescence was assessed with the IVIS Spectrum imaging system. (B) Bioluminescence measurements in mice treated with CD19 CAR T cells. Data are means ± SEM from seven replicate mice per cohort. By T test statistics, *p = 0.0474 for CD19 GTN GO versus CD19 GTN PBS at 21 days; **p = 0.0069 for CD19 GTN GO versus CD19 GTN PBS at 28 days; p = 0.9800 for CD19 GTN GO versus CD19 GTN PBS at 35 days. (C) Tumor volume measurements in mice treated with CD19 CAR T cells. Data are means ± SEM from seven replicate mice per cohort. By T test statistics, p = 0.1013 for CD19 GTN GO versus CD19 GTN PBS at 35 days. (D) Bioluminescence measurements in mice treated with anti-EGFR (806) CAR T cells. Data are means ± SEM from seven replicate mice per cohort. **p = 0.0040 for 806 GTN GO versus 806 GTN PBS at 21 days; p = 0.1131 for 806 GTN GO versus 806 GTN PBS at 28 days; ***p = 0.0005 for 806 GTN GO versus 806 GTN PBS at 35 days. (E) Tumor volume measurements in mice treated with anti-EGFR (806) CAR T cells. Data are means ± SEM from seven replicate mice per cohort. *p = 0.0240 for 806 GTN GO versus 806 GTN PBS at 35 days.

We next evaluated the antitumor function of *CpNA*-expressing CAR T-cells, using our well-established human xenograft model of neuroblastoma. SY5Y xenografts establish an immune-suppressive tumor environment enriched with immune and metabolic checkpoints. Infused CAR T cells effectively traffic to SY5Y tumors.[38] Despite undergoing robust proliferation, their antitumor function is limited.[39] The experimental layout for testing the efficacy of anti-GD-2 CAR T cells in this model is illustrated in Figure S7A. *CpNA* -expressing, anti-GD-2 4-1BBsCAR-T cells were expanded over 9 days until rested. To establish xenografts, immunodeficient mice were intravenously (i.v.) injected with 0.5 × 10^6 Click Beetle Green Luciferase-expressing SY5Y tumor cells. To determine the influence of *CpNA* on CAR T cell potency, we infused, 0.75 × 10^6 GFP or *CpNA*-expressing CAR T cells and measured tumor size at regular intervals by bioluminescence imaging. As expected, SY5Y xenografts grew exponentially over time. Control T cells (no CAR) had minimal impact on tumor cell growth (Figure S7C). Overall tumor volume was significantly reduced in tumor-bearing mice infused with CAR infected T cells. However, overall tumor burden remained high in *CpNA*-expressing CARTs. The levels of circulating T cells were significantly less in the *CpNA* CAR group, suggesting that proliferation

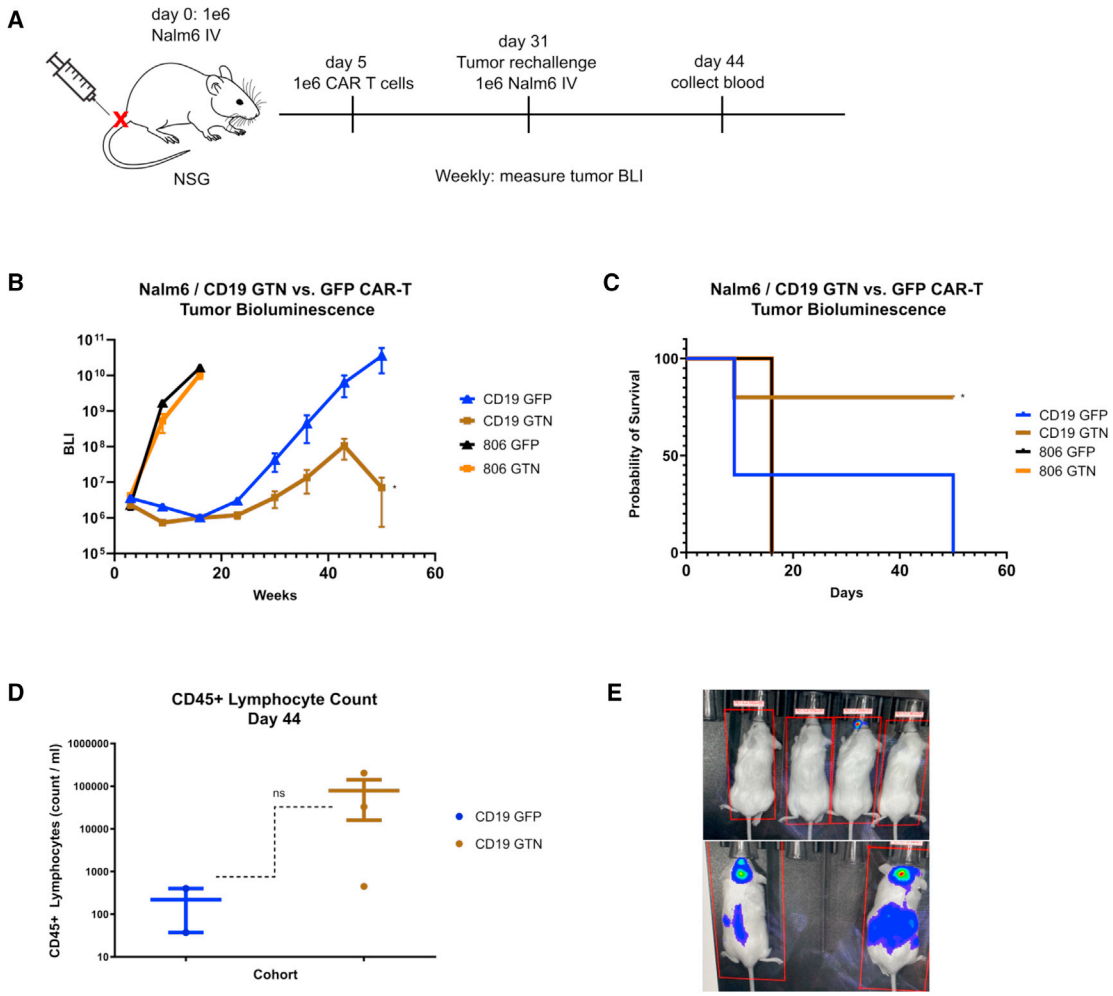

Figure 5. Targeting sialic acids with NA enhances CAR T cell antitumor function in the Nalm-6 xenograft model of leukemia

(A) NSG mice were infused by tail vein injection with 1 × 10^6 luciferase-expressing Nalm tumor cells (day 0). On day 5, the mice received 1 × 10^6 CAR T cells in PBS injected by tail vein. The CAR T cells expressed either tumor-targeting anti-CD19 CARs or irrelevant control 806 (EGFR-targeting) CARs, plus co-transduced GTN (*Cp*NA secreting) or GFP constructs. Every week, the tumor bioluminescence was assessed with the IVIS Spectrum imaging system. (B) Bioluminescence measurements in Nalm6 tumor-bearing mice treated with anti-CD19 or 806 CAR T cells either secreting *Cp*NA (GTN construct) or expressing GFP. Data are means ± SEM from starting cohorts of five mice per treatment arm. By two-way ANOVA, including all treatment arms, both time effect (*p = 0.0485) and treatment cohort effect (*p = 0.0226) were significant. A two-way ANOVA including only CD19 GTN and CD19 GFP arms showed significant time (*p = 0.0446), treatment (*p = 0.0163), and time × treatment interaction (***p < 0.0001) effects. (C) Survival proportions of Nalm6 tumor-bearing mice in each treatment cohort. Mice were killed if found to have BLI measurements over 1 × 10^{10} photon flux (p/s). Analysis with log rank (Mantel-Cox) testing demonstrated that the CD19 GTN and CD19 GFP survival curves are significantly different (*p = 0.0210). (D) Blood harvested on day 44 by retro-orbital puncture was stained with anti-human CD45 antibody in Truecount tubes (BD Biosciences) to detect adoptively transferred T cells. Data are CD45 + cells per mL of blood for individual mice plus cohort means ± SEM. By T test statistics with Welch's correction for unequal variances, the differences between CD19 GTN and CD19 GFP were not significant (p = 0.3372). (E) Images from final weekly measurement demonstrating BLI (photon flux intensity) of surviving mice, treated with either *Cp*NA secreting (top) or control GFP-expressing (bottom) CD19-directed CAR T cells.

was diminished following antigen exposure in this distinct microenvironment (Figure S7D). Overall effector function was compromised due to significantly lower CD8+ T cell numbers in the CAR *CpNA* group. SY5Y is a rapidly growing tumor and the aggressive nature of this malignancy limits the *in vivo* study to approximately 2 weeks. This is unsuited to approaches that offer therapeutic potential via enhanced persistence.

Conclusions

In this study, we engineered CAR T cells to secrete *C. perfringens* NA, hypothesizing that NA-expressing CAR Ts would have enhanced antitumor function by counteracting sialoglycan-mediated checkpoint pathways. We found that, *in vitro*, CAR T-secreted NA alone does enhance cytotoxicity against certain tumor lines during short-term co-culture assays. Moreover, *ex vivo* expanded T cells exposed

to NA activity have a more naïve-like ($CCR7^+$; $CD45RO^-$) differentiation profile. Less-differentiated CAR T products such as naive (Tn), stem cell memory (Tscm), and central memory T cells (Tcm) have more potent antitumor activity compared with effector or effector-memory differentiated T cells.[30–32] Correspondingly, the NA-secreting CAR T cells had enhanced persistence and more durable immunosurveillance within a tumor rechallenge model. One compelling model for T cell differentiation is that of "quorum sensing," in which interactions between clustering, primed T cells during a critical period determine their effector versus memory differentiation fate. Surface intercellular receptors including the integrin LFA-1 have been demonstrated to transmit differentiating signals between T cells.[40] Treatment with NA has been used for decades in research to promote rosette formation and contact between immune cells and targets.[41,42] On microscopy, there is generally a relative absence of unengaged, bystander T cells when NA is included in the media; virtually all T cells are involved in rosettes. These results suggest a model in which sialic acid removal influences T cell intercellular contact and therefore differentiation fate. Therapeutic strategies that target the immunomodulatory functions of sialic acids may also benefit from polarizing adoptive T cell products to a naïve-like phenotype.

Our findings regarding the CD2:CD58 axis are intriguing, because recent research has demonstrated the importance of the CD58 ligand in tumor immunosurveillance. Diverse tumor types can gain resistance to T and natural killer cell-mediated cytotoxicity through loss of CD58 expression.[43–45] Majzner et al. demonstrated that large B cell lymphomas (LBLCs) with aberration of CD58 had only a 25% rate of complete response with CAR T therapy compared with 82% for CD58-intact tumors.[44] The finding that the NA and GO combination requires CD58 for mitogenic signaling could provide a non-genetic approach to assay for the functional expression of this ligand on tumor cells. Importantly, our findings regarding the CD2:CD58 axis do not extend the known immune potentiating mechanisms of NA alone, as the presence of GO is required in addition to NA for this phenomenon.

We sought to boost the effect of NA by testing it in combination with a second glyco-active enzyme, GO, which can oxidize galactose residues exposed by NA. The combination of secreted NA and exogenous GO does enhance T cell polyfunctionality and nonspecific cytotoxicity *in vitro*. Mechanistically, the enzyme combination relies on the CD2:CD58 signaling axis to induce stimulatory effects. Results from our xenograft models of GBM, as well as our syngeneic model of B16 melanoma, however, show that NA alone enhances CAR T cell antitumor function *in vivo*, but when combined with GO, the subset of CAR Ts secreting NA demonstrates inferior tumor control. By distinguishing the relative importance of NA versus GO as adjuvants for CAR T cell therapies, we provide novel evidence that arming CAR T cells with NA enhances immunotherapeutic activity.

Our findings suggest possible mechanisms for the failure of injected GO to further enhance the performance of CAR T cells secreting NA *in vivo*. In the presence of both enzymes, T cells broadly react to targets expressing CD58. When applied to a co-culture assay, the effect of the enzyme combination leads to greater engagement of effectors (particularly nontransduced T cells) with tumor targets. Within the animal models, however, the enzyme combination may misdirect CAR T cells toward antigen-negative but CD58-positive bystander cells, effectively reducing the effector to tumor target ratio. Therefore, the success of the combination in co-culture assays may be an artifact of the lack of cellular diversity *in vitro*, with absent stromal and benign host cells that one would find in the tumor microenvironment. An alternative but not mutually exclusive hypothesis is that the stimulatory signal of the enzyme combination may be supraphysiologic and facilitate T cell exhaustion, an effect that may not be apparent in short-term co-culture assays but would be revealed in longer term animal studies. The calcium-calcineurin-NFAT signaling axis in T cells provides a link between excessive activation signals and an exhausted phenotype, and this effect could be at work in our *in vivo* findings of the NA and GO combination.[46]

In the design of combination immunotherapies, proteins that act on immune cell and tumor glycoproteins have been underexplored. Here, we use a nonnative enzyme, *CpNA*, to directly target surface glycans that suppress T cell function. Arming CAR T cells with *CpNA* confers superior efficacy and durability across a wide range of tumor models. Interestingly, we observed a striking T cell intrinsic benefit of *CpNA*. We show that NA shifts the differentiation of T cells into a naïve-like state, culminating in increased persistence and sustained tumor control *in vivo*. Our work addresses an immediate challenge and important priority for the clinical domain. Future work will be directed toward defining the role of *CpNA* in T cell differentiation. Such studies will shed light on sialic acids as a regulatory parameter influencing T cell fate.

MATERIALS AND METHODS

Tumor cell lines and culture

The human GB cell lines U87 and U251 and human B cell leukemia cell line Nalm6 were acquired from the American Type Culture Collection (ATCC). The tumor cell lines were transduced to stably express the CBG and eGFP under control of the EF-1α promoter. The cells were sorted on an Influx cell sorter (BD Biosciences) 3 days after transduction to be 100% GFP positive. The GB cell lines were maintained in Improved MEM Zinc Option (Gibco) with 10% fetal bovine serum (FBS) and 1% each of penicillin-streptomycin, GlutaMAX, HEPES, and sodium pyruvate. The Nalm6 cells were maintained in RPMI (Corning) with 10% FBS and 1% each of penicillin-streptomycin and HEPES.

Lentiviral production

The lentiviral vector pELNS-GFP_T2A_NA (GTN) encodes eGFP and *C. perfringens* NA separated by a T2A self-cleaving peptide and under the transcriptional control of EF-1 α. Lentiviral supernatants were generated by transient transfection of 293-T cells with pELNS-GFP_T2A_NA. 293-T cells were initially seeded in T150 flasks and grown to 80% confluence in 25 mL of culture medium (RPMI1640); 90 μL Lipofectamine 2000 DNA transfection reagent was combined with 7 μg pCL-VSVG, 18 μg pRSV-REV, and 18 μg

of pGAG-POL (Nature Technology) as well as 15 μg of pELNS-GFP_T2A_NA. This mixture was incubated at room temperature for 15 min. DNA-Lipofectamine complexes were then added to the 293-T cells.

After 24 h, infectious supernatants were sterile filtered through a 0.45-μm syringe tip cellulose acetate filter and collected in a 50-mL conical tube. To pellet the lentivirus, the supernatant was spun in a Thermo Fisher Scientific Centrifuge (LYNX 4000) at 18,000 RCF, overnight, at 4°C. The supernatant was removed, and the lentiviral pellet was resuspended in 1.6 mL of culture medium, aliquoted, and stored at −80°C. Generation of the 806 CAR, CD19 CAR, and eGFP encoding lentiviral particles followed the same procedure.

In vitro T cell transduction and expansion

Primary human leukocytes (PBLs) from healthy male and female volunteers were collected at the University of Pennsylvania's Apheresis Unit. Informed consent was obtained from all participants before collection. All experimental procedures and methods were approved by the University of Pennsylvania Institutional Review Board. T cells were purified at the University's Human Immunology Core by negative selection using the RosetteSep T cell enrichment cocktail (Stemcell). The T cells were activated overnight with anti-CD3/CD28 beads (Thermo Fisher Scientific). Populations of the cells were then transduced with lentiviral vectors for 806 CAR, CD19 CAR, GFP, or GTN constructs. The cells were expanded in complete RPMI Media (Corning), and after 10 days were frozen in aliquots and thawed as needed for experiments.

Cytotoxicity assay

The ability of CAR T cells co-transduced with GTN or GFP to kill tumor targets was tested in a luciferase-based cytotoxicity assay. CBG-expressing U87 cells (20×10^3) were cultured overnight in a 96-well microplate (Corning). The following day, CAR+ T cells were added to each well at E:T ratios of 10:1, 3:1, 1:1, and 1:3. Recombinant NA and GO (Millipore Sigma) were added in PBS to certain wells to final concentrations of 50 mU/mL and 375 mU/mL, respectively, while other wells received vehicle. Each condition was repeated in triplicate. After 24 h, luciferin in PBS was added to each well for a final concentration of 150 μg/mL. Bioluminescence was recorded with a Synergy HTX plate reader (BioTek).

Flow cytometry

For knockout studies, cell-surface protein expression was assessed using the following antibodies: anti-CD2–APC [RPA-2.10], anti-CD28–APC [CD28.2], anti-CD58–APC [TS2/9], anti- TRAC/TRBC–APC [IP26] (BioLegend). For anti-EGFR CAR expression, cells were incubated with recombinant EGFRvIII-Fc (Novus Biologicals) followed by polyclonal APC-conjugated anti-Fc secondary (Jackson ImmunoResearch). The anti-CAR19 idiotype for surface expression of CAR19 was provided by Novartis. The expression of murine CD45.1 was assessed with anti-mCD45.1–APC [A20] (Biolegend). In all cases, cells were washed with PBS, incubated with antibodies at room temperature for 30 min in buffer consisting of PBS, 1% BSA, and 5 mM EDTA, washed twice in PBS (or stained with secondary if indicated and washed), and evaluated on a BD LSR Fortessa. Analysis was performed using FlowJo software (Tree Star Inc. version 10.1).

Enzyme-linked immunosorbent assay

Target-expressing cells (20×10^3 U87 per well) were cultured overnight in a 96-well V-bottom plate. Thawed and rested CAR T cells were added at an E:T ratio of 1:1. The conditions included the following: CAR T cells, CAR T cells with NA secretion and GFP expression, and CAR T cells with GFP expression alone. The enzymes NA and GO were added at final concentrations of 50 mU/mL and 375 mU/mL, respectively, to appropriate wells as indicated in figure legends. All conditions were performed in triplicate. After 20 h, supernatants were removed, and the cytokines IFN-γ and IL-2 were quantified by Duoset ELISA (R&D Systems).

Neuraminidase activity assay

U87 and Nalm6 target cells (20×10^3 per well) were cultured overnight in a 96-well V-bottom plate. Thawed and rested CAR T cells co-transduced with GTN or GFP were washed once in fresh media and then added at a 10:1 ratio of GFP+ cells to target cells. After 24 h, the plate was centrifuged at $500 \times g$ for 3 min, and supernatants were tested for NA activity using the Fluorometric – Blue Neuraminidase Assay Kit (Abcam) per the manufacturer's protocol.

In vivo models

All mouse experiments were conducted in according to IACUC-approved protocols. Using NSG mice, 250×10^3 U87-luc-eGFP cells were injected subcutaneously in the right flank, with seven mice per group. For each injection, the tumor cells were suspended in in 100 μL of 20% Matrigel in PBS. One week after tumor implantation, the animals were injected i.v. via tail vein with 0.5×10^6 EGFR or CD19-directed CAR T cells, either secreting *Cp*NA or not as indicated in the figures. On a weekly basis, anesthetized mice were imaged using a Xenogen IVIS Spectrum system (Caliper Life Science) to assess tumor bioluminescence. Total bioluminescent flux was quantified using Living Image 4.4 (PerkinElmer). Tumor volumes were assessed via caliper measurement.

In the Nalm6 leukemia model, NSG mice were infused with 1×10^6 Nalm6-luc-eGFP tumor cells on day 0. On day 5, the mice received either *Cp*NA secreting or GFP-expressing CAR T infusions by tail vein injection, with five mice per cohort. Bioluminescence was evaluated weekly with the IVIS Spectrum imager as in the U87 experiment. On day 31, mice were re-challenged with an additional 1×10^6 tumor cells. Bloods were collected into Trucount tubes by cheek bleed procedure on day 44, stained for human CD45, and evaluated by flow cytometry to quantify the engrafted adoptive cells in the peripheral blood.

For the syngeneic mouse melanoma model, 50×10^3 B16F10.CD19 melanoma cells expressing human CD19 were implanted subcutaneously on the right flank in CD45.2 + C57BL/6 mice (The Jackson Laboratory), with seven mice per treatment arm. To generate CAR T cells, splenocytes were harvested from CD45.1 + congenic donor mice, from which T cells were isolated using the EasySep Mouse T cell

Isolation Kit (Stemcell Technologies), activated with Dynabeads Mouse T-Activator CD3/CD28 beads, and transduced by spinfection with ecotropic retrovirus encoding the CD19-directed CAR, GTN, or GFP constructs. Prior to use of mouse CAR T cells, the expression of CAR, GFP, and functional NA were confirmed by flow cytometry or enzyme activity assay as previously described for human cells. Mice with evidence of tumor engraftment (tumor volume >50 mm^3) on day 5 were randomized to either CD19-directed CAR T (co-expressing *Cp*NA or GFP) or NTD cell infusions, which occurred on days 5 and 12, as well as intra-tumoral injections of NA and GO, GO, or PBS as described in the figures. Tumor volumes were measured weekly beginning on day 5 as well as at the end of the experiment on day 21. To assess CAR T engraftment, blood was collected on day 21 by cardiac puncture, stained with APC-conjugated anti-CD45.1 antibody (Biolegend, clone A20) in Trucount tubes (BD Biosciences), and evaluated with flow cytometry. Animals were euthanized at the end of the experiment or when they met prespecified endpoints according to the protocols.

For the GD-2 xenograft model, animals were injected via tail vein with 0.5×10^6 SY5Y- CBG tumor cells (ATCC) in 0.1 mL sterile PBS. On day 4, tumor engraftment was confirmed; 0.75×10^6 anti-GD2 CAR T cells or nontransduced NTD human T cells were injected i.v. in 100 μL of sterile PBS, 5 days after injection of SY5Y-CBG tumor cells. Anesthetized mice were imaged using a Xenogen IVIS Spectrum system (Caliper Life Science) twice a week. Mice were given an intraperitoneal injection of D-luciferin (150 mg/kg; Caliper Life Sciences). Total flux was quantified using Living Image 4.4 (PerkinElmer) by drawing rectangles of identical area around mice, reaching from head to 50% of the tail length. Peripheral blood was obtained by retro-orbital bleeding in an EDTA-coated tube, and blood was examined fresh for evidence of T cell engraftment, and differentiation, by flow cytometry using BD Trucount (BD Biosciences).

Animals were euthanized at the end of the experiment before showing signs of toxicity and before reaching signals higher than 1×10^{11} p/s total flux per mouse (in accordance with our Institutional Animal Care and Use Committee [IACUC] protocols).

T cell differentiation assay

Activated CAR T cells were expanded for 9 to 11 days and subsequently stained with a panel of monoclonal antibodies to assess differentiation. The following pre-titrated antibodies were used: anti-CCR7–FITC (clone 150,503; BD PharMingen); anti-CD45RO-PE (clone UCHL1), anti-CD8-H7APC (clone SK1; BD Biosciences); anti-CD4-BV605 (clone OKT4). 1×10^6 cells were immunostained as follows: cells were washed with PBS and stained for viability using LIVE/DEAD Fixable aqua (Molecular Probes) for 15 min, washed once, and resuspended in fluorescence-activated cell sorting (FACS) buffer consisting of PBS, 1% BSA, and 5 mM EDTA. Cells were then incubated with the above indicated antibodies for 30 min at room temperature. Samples were then washed three times with FACS buffer and fixed in 1% paraformaldehyde. Positively stained cells were differentiated from background using fluorescence-minus-one controls. Flow cytometry was performed on BD LSR Fortessa. Analysis was performed using FlowJo software (Tree Star version 10.1).

SUPPLEMENTAL INFORMATION

Supplemental information can be found online at https://doi.org/10.1016/j.ymthe.2021.11.014.

ACKNOWLEDGMENTS

We thank Drs. Carl June, Elizabeth Hexner, Gerald Linette, Don Siegel, and Stephen Bagley at the University of Pennsylvania, as well as Dr. Michael Dustin at the University of Oxford, for their helpful discussions. We also thank the Human Immunology, Flow Cytometry, and Stem Cell and Xenograft cores at the University of Pennsylvania. R.S.O. is supported by the NIH grant RO1CA226983-04. Research reported in this publication was also supported by the National Center for Advancing Translational Sciences of the National Institutes of Health under award number TL1TR001880 (J.S.D.), as well as a St. Baldrick's Foundation Scholar Award, National Blood Foundation Scientific Research Grant Award, and Office of the Assistant Secretary of Defense for Health Affair through the Peer Reviewed Cancer Research Program under Award No. W81XWH-20-1-0417 (S.G.). The content is solely the responsibility of the authors and does not necessarily represent the official views of the National Institutes of Health. This study was also funded, in part, by the Glioblastoma Translational Center of Excellence within The Abramson Cancer Center at the University of Pennsylvania.

AUTHOR CONTRIBUTIONS

J.S.D., Z.B., D.M.O., M.M., and R.S.O. designed the study. J.S.D., S.G., V.B., Z.B., D.M.O., M.M., and R.S.O. provided conceptual guidance. J.S.D., S.G., E.S., L.J., J.L., Z.B., and R.S.O. performed the experiments. J.S.D., Z.B., and R.S.O. analyzed the data. J.S.D. and R.S.O. wrote the manuscript. Z.B., S.G., and D.M.O. read and made comments on the manuscript.

DECLARATION OF INTERESTS

M.C.M. is an inventor on patent applications related to CAR technology and has received licensing royalties from Novartis corporation; S.G. and M.C.M. are inventors on patent applications related to methods of manufacturing CAR T cells. D.M.O., Z.B., L.J., R.T., and V.B. are inventors on patents related to CAR T cells that have been filed by the University of Pennsylvania. The other authors declare no financial or other conflicts of interest.

REFERENCES

1. Majzner, R.G., and Mackall, C.L. (2019). Clinical lessons learned from the first leg of the CAR T cell journey. Nat. Med. *25*, 1341–1355.
2. Murciano-Goroff, Y.R., Warner, A.B., and Wolchok, J.D. (2020). The future of cancer immunotherapy: microenvironment-targeting combinations. Cell Res. *30*, 507–519.
3. De Sousa Linhares, A., Leitner, J., Grabmeier-Pfistershammer, K., and Steinberger, P. (2018). Not all immune checkpoints are created equal. Front. Immunol. *9*, 1909.
4. Agrawal, B. (2019). New therapeutic targets for cancer: the interplay between immune and metabolic checkpoints and gut microbiota. Clin. Transl. Med. *8*, 1–13.
5. Dusoswa, S.A., Verhoeff, J., Abels, E., Méndez-Huergo, S.P., Croci, D.O., Kuijper, L.H., de Miguel, E., Wouters, V.M.C.J., Best, M.G., Rodriguez, E., et al. (2020).

Glioblastomas exploit truncated O-linked glycans for local and distant immune modulation via the macrophage galactose-type lectin. Proc. Natl. Acad. Sci. U S A *117*, 3693–3703.

6. Rodriguez, E., Boelaars, K., Brown, K., Eveline Li, R.J., Kruijssen, L., Bruijns, S.C.M., van Ee, T., Schetters, S.T.T., Crommentuijn, M.H.W., van der Horst, J.C., et al. (2021). Sialic acids in pancreatic cancer cells drive tumour-associated macrophage differentiation via the siglec receptors siglec-7 and siglec-9. Nat. Commun. *12*, 1–14.

7. Rodriguez, E., Schetters, S.T., and van Kooyk, Y. (2018). The tumour glyco-code as a novel immune checkpoint for immunotherapy. Nat. Rev. Immunol. *18*, 204–211.

8. Stanczak, M.A., Siddiqui, S.S., Trefny, M.P., Thommen, D.S., Boligan, K.F., von Gunten, S., Tzankov, A., Tietze, L., Lardinois, D., Heinzelmann-Schwarz, V., et al. (2018). Self-associated molecular patterns mediate cancer immune evasion by engaging siglecs on T cells. J. Clin. Invest. *128*, 4912–4923.

9. Ikehara, Y., Ikehara, S.K., and Paulson, J.C. (2004). Negative regulation of T cell receptor signaling by siglec-7 (p70/AIRM) and siglec-9. J. Biol. Chem. *279*, 43117–43125.

10. Büll, C., den Brok, M.H., and Adema, G.J. (2014). Sweet escape: sialic acids in tumor immune evasion. Biochim. Biophys. Acta *1846*, 238–246.

11. Cohnen, A., Chiang, S.C., Stojanovic, A., Schmidt, H., Claus, M., Saftig, P., Janßen, O., Cerwenka, A., Bryceson, Y.T., and Watzl, C. (2013). Surface CD107a/LAMP-1 protects natural killer cells from degranulation-associated damage. Blood *122*, 1411–1418. https://doi.org/10.1182/blood-2012-07-441832, https://www.ncbi.nlm.nih.gov/pubmed/23847195.

12. Khazen, R., Müller, S., Gaudenzio, N., Espinosa, E., Marie-pierre, P., and Valitutti, S. (2016). Melanoma cell lysosome secretory burst neutralizes the CTL-mediated cytotoxicity at the lytic synapse. Nat. Commun. *7*, 10823. https://doi.org/10.1038/ncomms10823, https://www.ncbi.nlm.nih.gov/pubmed/26940455.

13. Santegoets, K.C.M., Gielen, P.R., Büll, C., Schulte, B.M., Kers-Rebel, E.D., Küsters, B., Bossman, S.A.J.F.H., Ter Laan, M., Wesseling, P., and Adema, G.J. (2019). Expression profiling of immune inhibitory siglecs and their ligands in patients with glioma. Cancer Immunol. Immunother. *68*, 937–949.

14. Büll, C., Boltje, T.J., van Dinther, E.A., Peters, T., de Graaf, A.M., Leusen, J.H., Kreutz, M., Figdor, C.G., den Brok, M.H., and Adema, G.J. (2015). Targeted delivery of a sialic acid-blocking glycomimetic to cancer cells inhibits metastatic spread. ACS Nano *9*, 733–745.

15. Bekesi, J.G., Arneault, G.S., Walter, L., and Holland, J.F. (1972). Immunogenicity of leukemia L1210 cells after neuraminidase treatment. J. Natl. Cancer Inst. *49*, 107–118.

16. Bekesi, J.G., Roboz, J.P., and Holland, J.F. (1976). Therapeutic effectiveness of neuraminidase-treated tumor cells as an immunogen in man and experimental animals with leukemia. Ann. N. Y. Acad. Sci. *277*, 313–331.

17. Sedlacek, H.H., Hagmayer, G., and Seiler, F.R. (1986). Tumor therapy of neoplastic diseases with tumor cells and neuraminidase. Cancer Immunol. Immunother. *23*, 192–199.

18. Miyagi, T., Wada, T., Yamaguchi, K., and Hata, K. (2003). Sialidase and malignancy: a minireview. Glycoconj. J. *20*, 189–198.

19. Gray, B.N., Walker, C., Andrewartha, L., Freeman, S., and Bennett, R.C. (1989). Controlled clinical trial of adjuvant immunotherapy with BCG and neuraminidase--treated autologous tumour cells in large bowel cancer. J. Surg. Oncol. *40*, 34–37.

20. He, D., Sun, L., Li, C., Hu, N., Sheng, Y., Chen, Z., Li, X., Chi, B., and Jin, N. (2014). Anti-tumor effects of an oncolytic adenovirus expressing hemagglutinin-neuraminidase of newcastle disease virus in vitro and in vivo. Viruses *6*, 856–874.

21. Zhou, Z., Wang, X., Jiang, L., Li, D., and Qian, R. (2021). Sialidase-conjugated "NanoNiche" for efficient immune checkpoint blockade therapy. ACS Appl. Bio. Mater. *4*, 5735–5741.

22. Hsieh, H., Calcutt, M.J., Chapman, L.F., Mitra, M., and Smith, D.S. (2003). Purification and characterization of a recombinant α-N-acetylgalactosaminidase from clostridium perfringens. Protein Expr. Purif. *32*, 309–316.

23. Moustafa, I., Connaris, H., Taylor, M., Zaitsev, V., Wilson, J.C., Kiefel, M.J., von Itzstein, M., and Taylor, G. (2004). Sialic acid recognition by vibrio cholerae neuraminidase. J. Biol. Chem. *279*, 40819–40826.

24. Seyrantepe, V., Landry, K., Trudel, S., Hassan, J.A., Morales, C.R., and Pshezhetsky, A.V. (2004). Neu4, a novel human lysosomal lumen sialidase, confers normal phenotype to sialidosis and galactosialidosis cells. J. Biol. Chem. *279*, 37021–37029.

25. Rajendran, M., Nachbagauer, R., Ermler, M.E., Bunduc, P., Amanat, F., Izikson, R., Cox, M., Palese, P., Eichelberger, M., and Krammer, F. (2017). Analysis of anti-influenza virus neuraminidase antibodies in children, adults, and the elderly by ELISA and enzyme inhibition: evidence for original antigenic sin. MBio *8*, 2281.

26. Novogrodsky, A., and Katchalski, E. (1973). Induction of lymphocyte transformation by sequential treatment with neuraminidase and galactose oxidase. Proc. Natl. Acad. Sci. U S A *70*, 1824–1827.

27. Novogrodsky, A. (1975). Induction of lymphocyte cytotoxicity by modification of the effector or target cells with periodate or with neuraminidase and galactose oxidase. J. Immunol. *114*, 1089–1093, http://www.jimmunol.org/cgi/content/abstract/114/3/1089.

28. Rhodes, J., Zheng, B., and Morrison, C.A. (1995). Galactose oxidation as a potent vaccine adjuvant strategy. efficacy in murine models and in protection against a bovine parasitic infection. Ann. N. Y. Acad. Sci. *754*, 169.

29. Reinhard, K., Rengstl, B., Oehm, P., Michel, K., Billmeier, A., Hayduk, N., Klein, O., Kuna, K., Ouchan, Y., Wöll, S., et al. (2020). An RNA vaccine drives expansion and efficacy of claudin-CAR-T cells against solid tumors. Science *367*, 446–453.

30. Gattinoni, L., Klebanoff, C.A., Palmer, D.C., Wrzesinski, C., Kerstann, K., Yu, Z., Finkelstein, S.E., Theoret, M.R., Rosenberg, S.A., and Restifo, N.P. (2005). Acquisition of full effector function in vitro paradoxically impairs the in vivo antitumor efficacy of adoptively transferred CD8 T cells. J. Clin. Invest. *115*, 1616–1626.

31. Berger, C., Jensen, M.C., Lansdorp, P.M., Gough, M., Elliott, C., and Riddell, S.R. (2008). Adoptive transfer of effector CD8 T cells derived from central memory cells establishes persistent T cell memory in primates. J. Clin. Invest. *118*, 294–305.

32. Alizadeh, D., Wong, R.A., Yang, X., Wang, D., Pecoraro, J.R., Kuo, C.F., Aguilar, B., Qi, Y., Ann, D.K., Starr, R., et al. (2019). IL15 enhances CAR-T cell antitumor activity by reducing mTORC1 activity and preserving their stem cell memory phenotype. Cancer Immunol. Res. *7*, 759–772.

33. O'Rourke, D.M., Nasrallah, M.P., Desai, A., Melenhorst, J.J., Mansfield, K., Morrissette, J.J.D., Martinez-Lage, M., Brem, S., Maloney, E., Shen, A., et al. (2017). A single dose of peripherally infused EGFRvIII-directed CAR T cells mediates antigen loss and induces adaptive resistance in patients with recurrent glioblastoma. Sci. Transl. Med. *9*, eaaa0984. https://doi.org/10.1126/scitranslmed.aaa0984, https://www.ncbi.nlm.nih.gov/pubmed/28724573.

34. Ocklind, G., Talts, J., and Lindahl-Kiessling, K. (1988). Activation of human T cells by neuraminidase-galactose oxidase-treated erythrocytes involving CD2 (T11) and its complementary structure. Scand. J. Immunol. *27*, 697–704.

35. Sanjana, N.E., Shalem, O., and Zhang, F. (2014). Improved vectors and genome-wide libraries for CRISPR screening. Nat. Methods *11*, 783–784.

36. Bajnok, A., Ivanova, M., Rigó, J., and Toldi, G. (2017). The distribution of activation markers and selectins on peripheral T lymphocytes in preeclampsia. Mediators Inflamm. *2017*, 8045161.

37. Kaizuka, Y., Douglass, A.D., Vardhana, S., Dustin, M.L., and Vale, R.D. (2009). The coreceptor CD2 uses plasma membrane microdomains to transduce signals in T cells. J. Cell Biol. *185*, 521–534.

38. Sellmyer, M., Richman, S., Lohith, K., Hou, C., Lieberman, B., Mankoff, D., Mach, R., Milone, M., and Farwell, M. (2018;59:122). In vivo monitoring of CAR T cells using [18F] fluoropropyl-trimethoprim. Mol. Ther.

39. Ghassemi, S., Martinez-Becerra, F.J., Master, A.M., Richman, S.A., Heo, D., Leferovich, J., Tu, Y., García-Cañaveras, J.C., Ayari, A., et al. (2020). Enhancing chimeric antigen receptor T cell anti-tumor function through advanced media design. Mol. Ther. Methods Clin. Dev. *18*, 595–606.

40. Gérard, A., Khan, O., Beemiller, P., Oswald, E., Hu, J., Matloubian, M., and Krummel, M.F. (2013). Secondary T cell–T cell synaptic interactions drive the differentiation of protective CD8 T cells. Nat. Immunol. *14* (4), 356–363.

41. Galili, U., and Schlesinger, M. (1974). The formation of stable E rosettes after neuraminidase treatment of either human peripheral blood lymphocytes or of sheep red blood cells. J. Immunol. *112*, 1628–1634.

42. Weiner, M.S., Bianco, C., and Nussenzweig, V. (1973). Enhanced binding of neuraminidase-treated sheep erythrocytes to human T lymphocytes. Blood *42*, 939–946.

43. Challa-Malladi, M., Lieu, Y.K., Califano, O., Holmes, A.B., Bhagat, G., Murty, V.V., Dominguez-Sola, D., Pasqualucci, L., and Dalla-Favera, R. (2011). Combined genetic inactivation of β2-microglobulin and CD58 reveals frequent escape from immune recognition in diffuse large B cell lymphoma. Cancer Cell *20*, 728–740.

44. Majzner, R.G., Frank, M.J., Mount, C., Tousley, A., Kurtz, D.M., Sworder, B., Murphy, K.A., Manousopoulou, A., Kohler, K., Rotiroti, M.C., et al. (2020). CD58 aberrations limit durable responses to CD19 CAR in large B cell lymphoma patients treated with axicabtagene ciloleucel but can be overcome through novel CAR engineering. Blood *136*, 53–54.

45. Frangieh, C.J., Melms, J.C., Thakore, P.I., Geiger-Schuller, K.R., Ho, P., Luoma, A.M., Cleary, B., Jerby-Arnon, L., Malu, S., Cuoco, M.S., et al. (2021). Multi-modal pooled perturb-CITE-seq screens in patient models define novel mechanisms of cancer immune evasion. Nat. Genet. *53*, 332–341.

46. Hogan, P.G. (2017). Calcium–NFAT transcriptional signalling in T cell activation and T cell exhaustion. Cell Calcium *63*, 66–69.